Structural Design and Modular Construction Approach For the Mk1 PB-FHR

NE 170 – Senior Design Project

This report presents design work performed by
Sea Hong, Jaben Root, Huu Duy Nguyen, and Daisuke Kazama
Department of Nuclear Engineering
University of California, Berkeley

With special thanks to Bernd Laskewitz (Westinghouse), Per Peterson (UCB), Joe Bower (UCB), Tom Caine (GE Vallecitos), and all other Subject Matter Experts who contributed to the intellectual advice and guidance provided in the research leading to the accumulation of material which is in this report.

June 20th, 2014

ABSTRACT

This report presents a comprehensive assessment, using a literature review and expert elicitation, to identify the major systems needed for the Mark 1 pebble-bed fluoride-salt-cooled, high-temperature reactor (Mk1 PB-FHR) to function. The design team identified functional requirements and determined the size of equipment needed to perform these functions. Because no design information was available for the polar crane and the direct reactor auxiliary cooling system modules for passive decay heat removal, the team developed designs for these systems. The team then developed a design for the Mk1 PB-FHR reactor building to integrate these systems into the cylindrical shield building and air duct vaults, and developed a detailed 3-D computer aided design model for the reactor building and its contents, using the same steel-plate composite structures used in the Westinghouse AP1000 reactor. The team used this 3-D plant model to estimate the inventories of key structural materials (steel and concrete) needed to construct the Mk1 PB-FHR building and to develop and assess a modular construction approach using the same methods and module manufacturing infrastructure as the AP1000. The team developed a storyboard for the construction process, showing how a lift tower would be used to install modules and equipment, and how economies can be achieved by sequential construction of reactors at a 12-unit site. The team also provides recommendations for approaches to further improve the reactor design.

CONTENTS

1.0 INTRODUCTION

The University of California, Berkeley (UCB) has been developing technology to couple fluoride-salt-cooled, high-temperature reactors (FHRs) to conventional air-Brayton combined cycle power plants (Andreades et al., 2014). The Mark 1 pebble-bed FHR (Mk1 PB-FHR) is a 236-MWt FHR preconceptual design developed at UCB that couples to a General Electric 7FB gas turbine with a heat recovery steam generator (HRSG) and steam bottoming cycle. The Mk1 design is capable of producing 100 MWe using only nuclear heat, and can peak between 100 and 242 MWe using gas co-firing. Figure 1.1 shows the configuration of the reactor, main salt piping, coiled tube air heaters (CTAHs), air ducts and power conversion system developed for the Mk1 PB-FHR design.

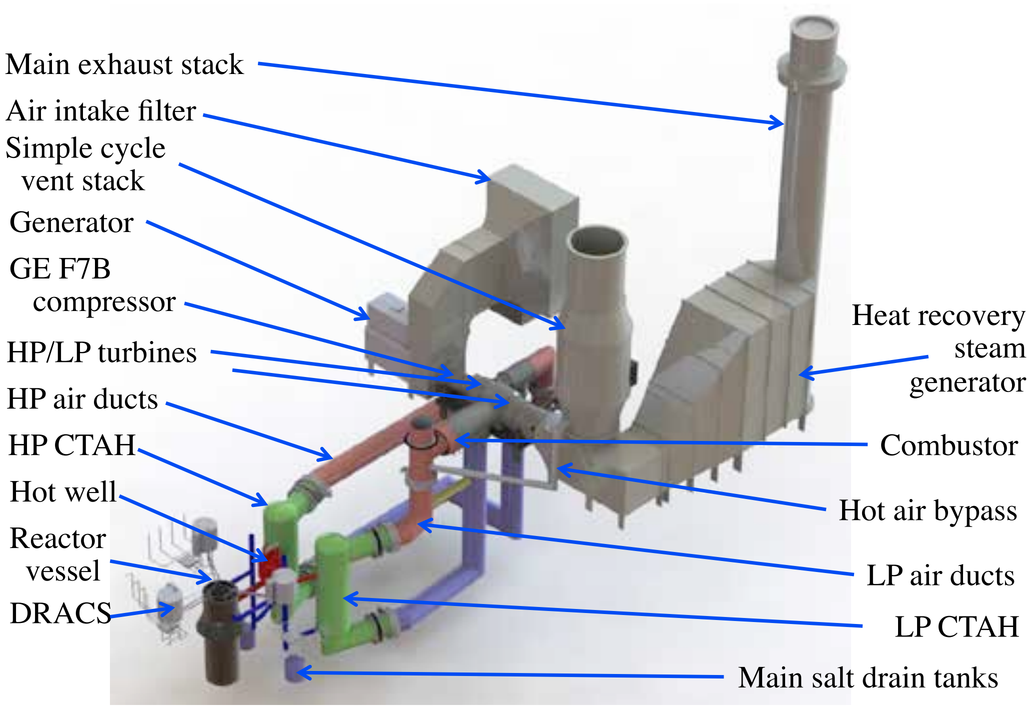

Fig. 1.1 The Mk1 PB-FHR reactor, main salt piping, CTAHs, and power conversion system (Andreades et al., 2014).

The configuration of the Mk1 PB-FHR places the reactor and CTAHs slightly below grade, and allows the reactor building to be separated from the power conversion system so the reactor can be located inside the plant protected area, while the power conversion system is in the owner-controlled area that requires a lower level of physical protection. This report describes work by the Mk1 Design Integration team to develop the design of a cylindrical shield building to enclose major Mk1 reactor systems, as well as a below-grade air duct vault to connect the CTAHs to the power conversion system.

To "wrap" a shield building around the Mk1 reactor, the Design Integration team considered a range of issues. First, it identified the additional major systems that are needed inside the shield building, as well as the major functional requirements of these systems, and developed a physical arrangement for the building to provide appropriate space and access for these systems. This included coordinating closely with the Fuel

Handling design team (Cho et al., 2014). Second, the team established reasonable design parameters for the Mk1 shield building dimensions, particularly the shield building wall and base mat thicknesses, using scaling from the Westinghouse AP1000 cylindrical shield building design. Here the team gratefully acknowledges scaling advice provided by Dr. Bernd Laskewitz, who is an expert in structural engineering and is familiar with the AP1000 design. The team also gratefully acknowledges Tom Caine from GE Vallecitos, who allowed the team to tour their hot-cell facilities and to learn about nuclear facility design. Third, the team considered key issues related to containment, ventilation, maintenance, equipment installation and replacement, and radiation protection. In designing the reactor building for radiation protection, the team coordinated closely with the Radiation Protection team (Chauduri et al., 2014). Finally, the Mk1 shield building uses modular, steel-plate/concrete composite (SC) construction methods quite similar to those used in the AP1000 reactor. Therefore, the team anticipates that these modules can be manufactured in the same factories that produce AP1000 modules using computer-aided manufacturing today, and will use similar design principles.

The modular design of the Mk1 reactor facility provides a revolutionary concept in the development of new nuclear facilities and a technology to greatly reduce the carbon emissions and fuel costs of natural gas combined cycle plants, while maintaining their flexibility to provide valuable grid support services including peaking power, spinning reserve, and frequency regulation. The Mk1's advanced design features, both in construction and flexible power production, could truly change the nature of the nuclear power industry. The Mk1 may allow for a much faster construction time of individual modules compared to the AP1000 and offer a much lower entry level investment for the initial module, while providing the possibility of further expansion in power generation. The Mk1 design will provide a modular construction capability to allow the development or expansion of a current operating site, which allows the implementation of multiple Mk1 reactors at one site. Because the Mk1 can produce both base-load and peaking power, the 12-unit station design considered here can produce 1200 MWe in base-load, and ramp rapidly to 2900 MWe using natural gas co-firing when peak power is needed.

This groundbreaking 12-unit station concept will not only provide power companies with the ability to replace aging fossil power plants with Mk1 systems, but also to expand their energy production capabilities by deploying additional modules on site. The Mk1 enjoys a symbiotic relationship with intermittent renewable energy sources in that it can expand low-carbon base-load power generation while also driving the efficiency of peak power generation up greatly. With this in mind, the development of the Mk1's systems has implemented design features that allow for modular construction to allow multiple Mk1 systems to be deployed at a flexible rate to meet varying load growth demands.

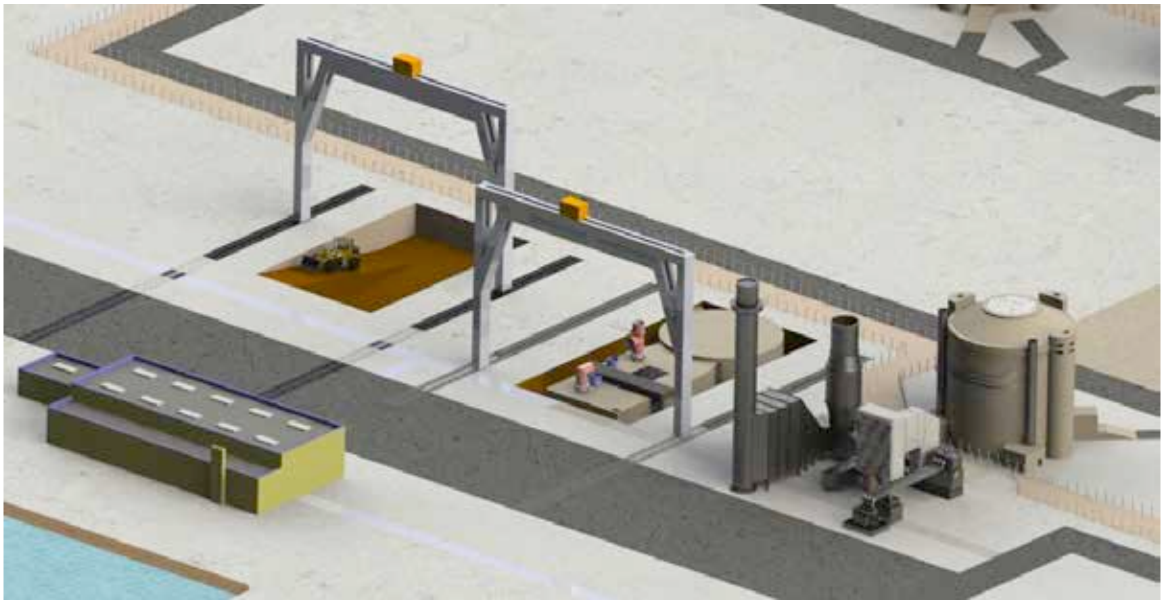

Fig. 1.2 Mk1 PB-FHR power plant units developed by the Design Integration team, with a module in start-up testing (right) adjacent to two units in construction. The common steam turbine building for four units is to the left.

Figure 1.2 depicts a Mk1 unit in operation, with two additional units starting construction alongside. The separate and independent nature of each unit allows for the simultaneous operation of the completed units while the subsequent units are being installed. All design features taken into account in the development of this plant model are discussed in the following sections of this report.

2.0 Mk1 REACTOR BUILDING DESIGN AND CONSTRUCTION METHODOLOGY

The Design Integration team was asked to develop a modular design for the shield building and air duct vault for the Mk1 PB-FHR reactor and power conversion systems shown in Fig. 1.1. The goal was to use the same modular construction infrastructure as is used for the AP1000, but to redesign the SC modules to be optimized for the Mk1 design. Another goal was to design a modest number of modules, fabricated from submodules, so that site assembly of the Mk1 units can use the same methods (but with smaller cranes) as the AP1000.

This chapter summarizes the Mk1 reactor building that we developed, and the ideas behind its design, using numerous computer-aided design figures. Figure 2.1 shows the baseline Mk1 site arrangement that we were provided at the beginning of this project. This baseline site has 12 Mk1 reactor units, as well as a variety of support services. This Mk1 station would be capable of producing 1200 MWe of base-load electricity without any carbon emissions, and has the flexibility to peak up to 2900 MWe with an efficiency level of 66% in converting natural gas or hydrogen into electricity. We were also asked to develop a reactor modular design and construction strategy that would be able to use the existing AP1000 module fabrication infrastructure and would allow modules to be built with high efficiency, so that construction crews responsible for specific construction tasks (excavation, module welding, equipment installation, module transport and emplacement, concrete pouring, etc.) have the opportunity to learn-by-doing for the first two modules and to use lessons learned to improve construction efficiency for the next 10 units.

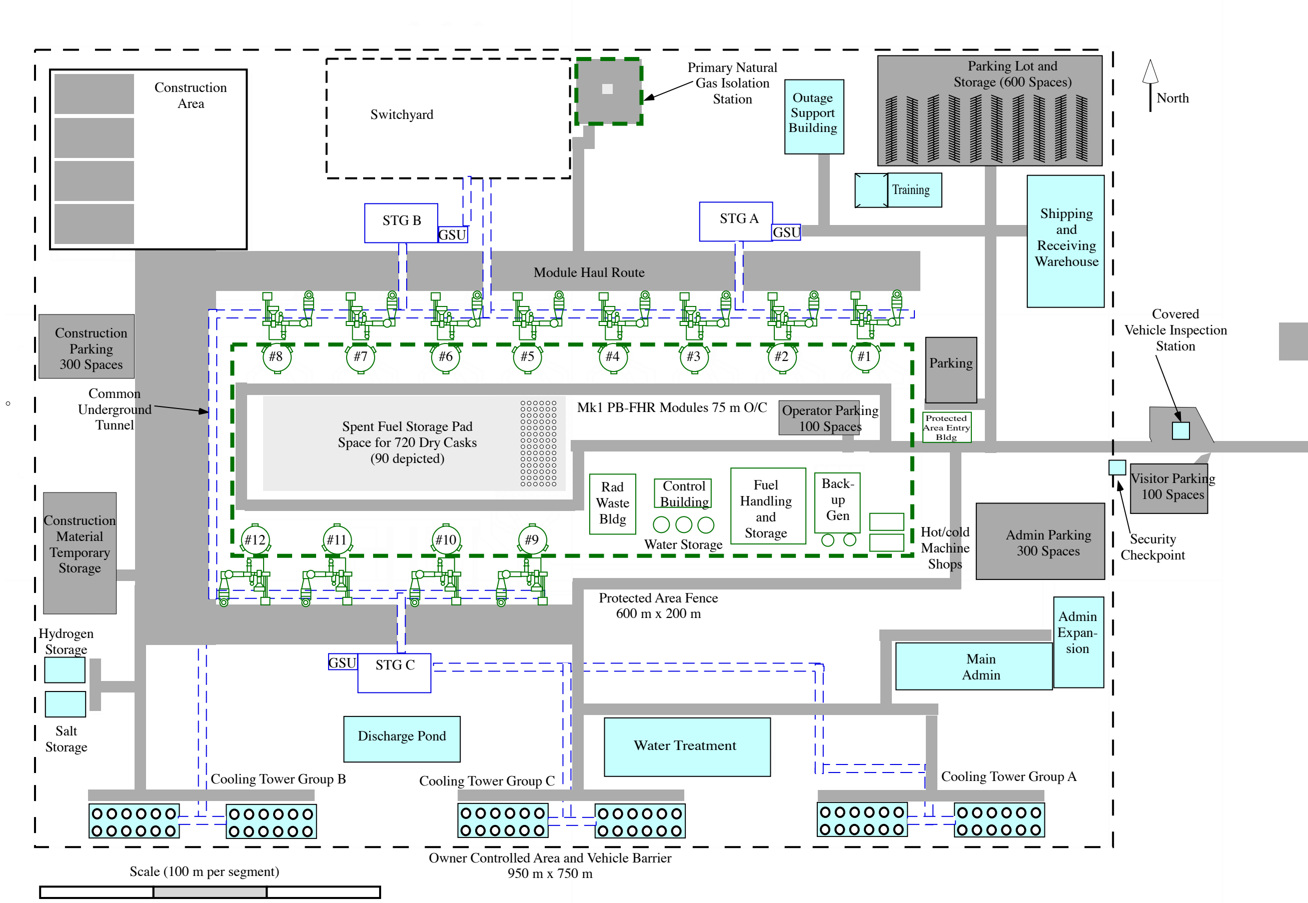

Fig 2.1 The baseline 1200-MWe base-load, 2900-MWe peak Mk1 site arrangement (Andreades et al., 2014), showing the locations of 12 Mk1 units, the protected area fence, and the construction area where Mk1 structural modules are fabricated.

2.1 Mk 1 Design and Construction

In this section, we provide a step-by-step walkthrough of the major elements of work needed to build a Mk1 module. The Design Integration team started this project with a skeleton model, shown in Fig. 2.2, and was assigned the task of developing the key components and systems of a full reactor building design. The cylindrical structure acts as a shield building, which houses the key systems of the Mk1 that required design, including the direct reactor auxiliary cooling system (DRACS) for passive decay heat removal, with its exhaust chimneys, an air duct vault, an underground common utilities tunnel, a personnel airlock to provide access to the shield building, an equipment hatch, an auxiliary exhaust system, a fuel canister well and numerous additional structural features.

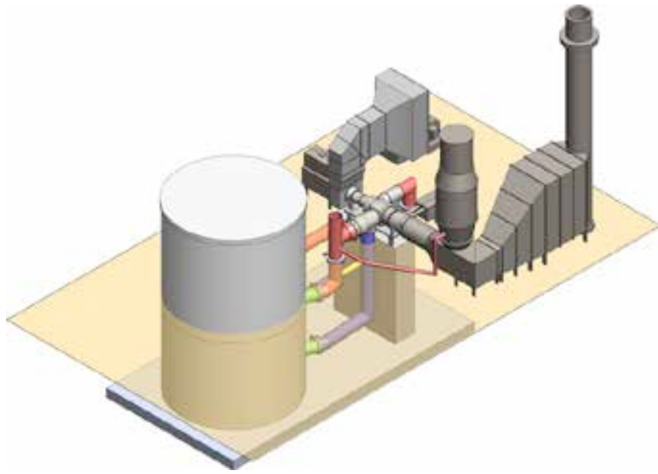

Fig 2.2 The Mk1 reactor building design before the Design Integration team started work, showing the initial concept of a cylindrical shield building.

2.2 Mk 1 Modular Construction Method

The Design Integration team has implemented a modular design in the development of the 10 modules used to construct a Mk1 reactor. A major goal of our design was to utilize existing AP1000 module fabrication factories to build Mk1 modules, which has been done using approximate scaling advice provided by Westinghouse. Figure 2.3 shows photos of SC structural modules being manufactured and shipped for AP1000 reactors in China. Because the factory fabrication of these modules uses the same computer-aided manufacturing methods as will be used for Mk1 modules, these factories can readily provide structural modules for Mk1 plants.

Fig. 2.3 Existing AP1000 module fabrication factories, as shown above, use computer-aided manufacturing and can also fabricate Mk1 modules (http://www.docin.com/p-98680862.html).

Similar to the AP1000, the Mk1 PB-FHR uses SC wall construction in which steel plates, shown in Fig. 2.4, are used to create both the pouring forms and the reinforcement for concrete. The use of modular prefabricated components will greatly reduce the cost of construction and transport of these plants, while also providing a technique that facilitates rapid construction from the design phase to operating conditions.

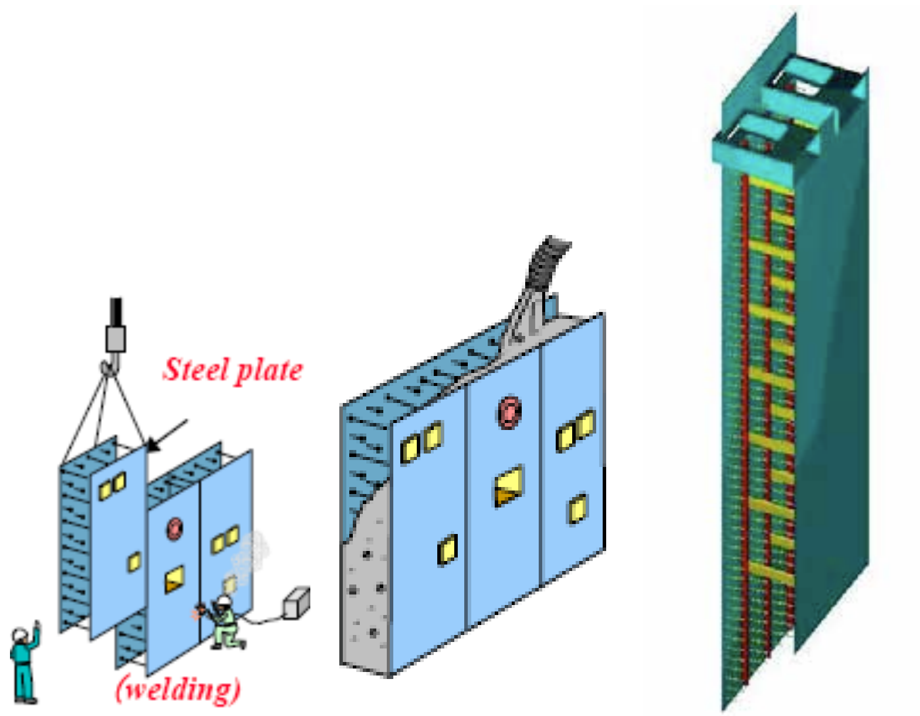

Fig 2.4 The technique and implementation of the modular steel-plate composite wall construction as used in the AP1000 (R. Matzie and J. Goossen, Westinghouse, May 12, 2008).

In the design of the Mk1 reactor unit, our team has relied on the proven modular construction method that Westinghouse has developed for the AP1000 while improving the technique to better suit the modular Mk1 construction method, which uses much larger numbers of smaller reactor modules. This method has been demonstrated in Sanmen, China, and more recently in the U.S., as shown by photos from the Vogtle and Summer sites in Fig. 2.5.

Vogtle Unit 3 shield building wall panels, May 2014

Summer Unit 2 CA20 Transported from MAB

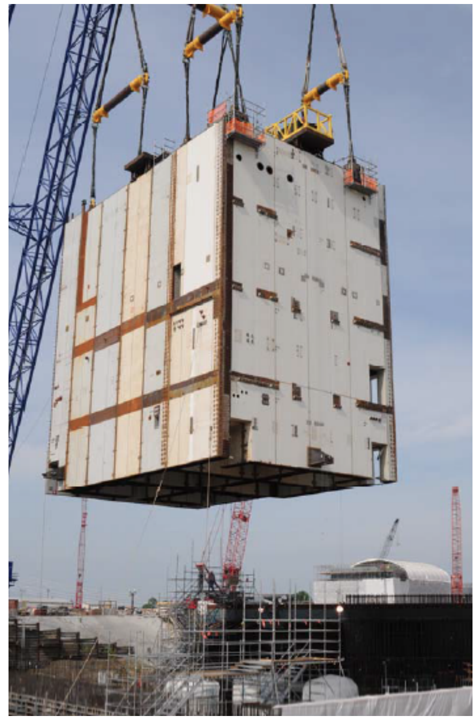

CA20 being set in place by heavy crane

Fig. 2.5 SC modular construction is being used now to build AP1000 reactors at the Vogtle (http://www.southerncompany.com/what-doing/energy-innovation/nuclear-energy/gallery/new/) and Summer (https://www.flickr.com/photos/scegnews/sets/72157629244341909/) sites in the U.S.

The largest structural module used in the Mk1 design weighs under 350 tons, less than half the weight of the largest AP1000 structural modules. As an improvement to Westinghouse's method for construction of the AP1000, our group developed a construction appraoch that can use a "lift tower" as opposed to a large crane. Currently, the thousand-ton cranes used to construct AP1000 reactors, as seen in Fig. 2.5, are among the largest in the world and require long lead times to be available. Besides being lighter, lift towers have the advantage of having better stability under high-wind conditions. Each Mk1 PB-FHR unit will be constructed from 10 structural modules. The 1150-MWe AP1000 uses some 350 modules, of which approximately one third are structural and the remainder are mechanical. Therefore, the 1200-MWe base-load Mk1 station, with 12 units, and with 9 or a few more structural modules per unit, uses only a slightly larger number of structural modules than a single AP1000.

Strutural modules are transported from covered buildings in the assembly area, like that shown in Fig. 2.6, using crawlers, to a pick-up pad adjacent to the unit being constructed. A Mk1 lift tower runs on a set of tracks to assemble the modules of the shield building and the air duct vault on the basemat. Concrete is poured into place after each module is set in place.

Fig. 2.6 A covered assembly area at the Sanmen, China site for the fabrication of modules for construction of a Westinghouse AP1000.

The plan for implementing this technique will take the assembled modules, which are moved by transporters to the pick-up area for the lift towers. It will also involve the use of common utility tunnels, which eliminate the need to have above-ground piping and electrical lines, simplifying transport of modules to their final location.

2.3 Mk 1 Modular Construction Approach

As noted above, the Mk 1 shield building and air duct vaults are assembled from 10 structural modules. Figure 2.7 shows the 10 structural modules, while Table 2.1 presents key design data for each module, as well as for other elements of the Mk1 system.

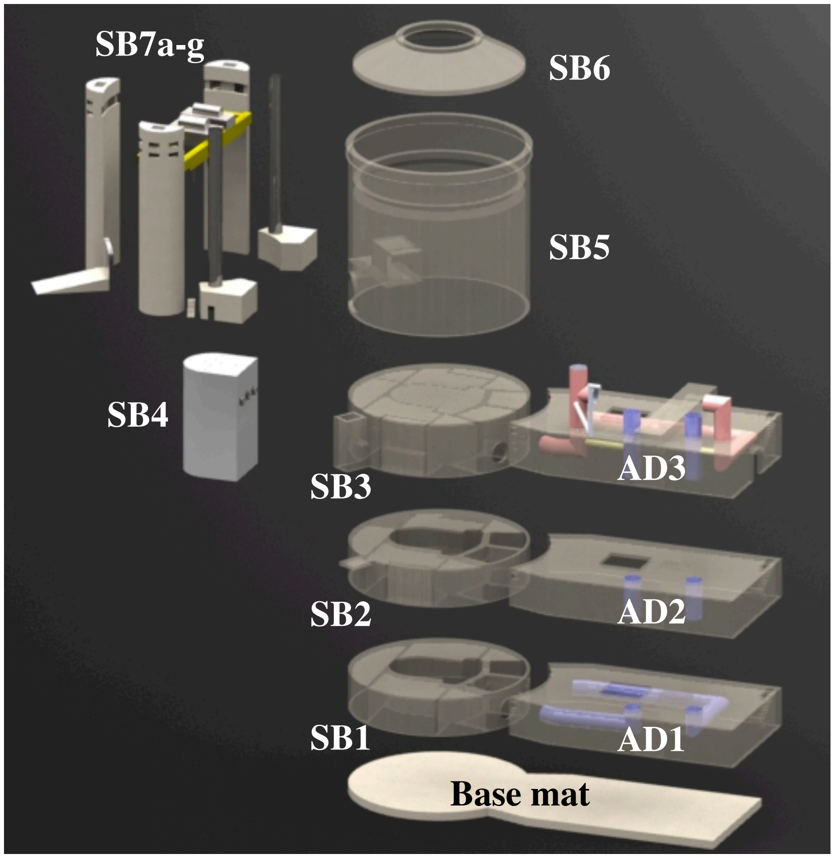

Fig. 2.7 Exploded view of the 10 structural modules used in the Mk1 reactor building developed by the Design Integration team.

Table 2.1. Mk1 design parameters for shield building and air duct vault structural and other modules.

	Width (m)	Length (m)	Height (m)	Steel Mass (1000 kg)	Concrete (1000 kg)
Base mat	25.0	56.16	1.2	336.8	3601.5
Shield building level 1 module SB1	25.0	25.0	5.5	163.8	1638.1
Shield building level 2 module SB2	25.0	25.0	5.5	163.8	2293.0
Shield building level 3 module SB3	25.0	25.0	7.78	202.6	2994.0
Reactor cavity structural module SB4	8.16	9.55	15.28	111.9	1674.0
Shield building upper ring SB5	25.0	25.0	24.65	598.8	3498.7
Polar crane	7	22.5	4.75	1055.6	0
Shield building roof SB6	23.7	23.7	4.67	166.0	680.2
Shield building external structures (DRACS chimneys, etc.)	-	-	-	305.8	1954.1
Air duct vault level 1 module AD1 †	18.77	33.70	5.50	258.2	1713.3
Air duct vault level 1 module AD2 †	18.77	33.70	5.50	180.6	1713.3
Air duct vault level 1 module AD3 †	18.77	33.70	6.28	335.4	2267.4
TOTALS				**3879**	**24027**

† Includes steel mass of 2.5-cm thick air duct pipes preinstalled in module.

The Design Integration team developed a concept for modular construction for Mk1 plants, that allows a new Mk1 unit to be constructed adjacent to an operating unit. Figure 2.8 provides a detailed storyboard showing the construction steps involved. The key idea is that all construction activities occur outside of the protected area of the plant, separated from the protected area by a temporary double fence system. When construction is complete, the permanent protected area fence is installed and the temporary fence removed, so the shield building is then inside the protected area and fuel can be loaded for startup testing.

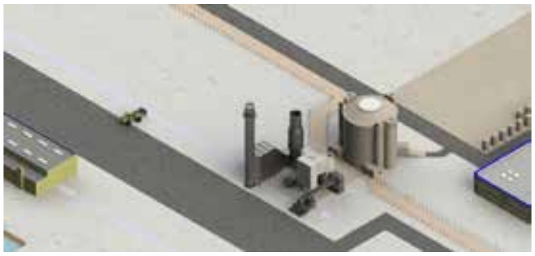

(1) Construction occurs adjacent to an existing Mk1 unit, outside a temporary PA fence

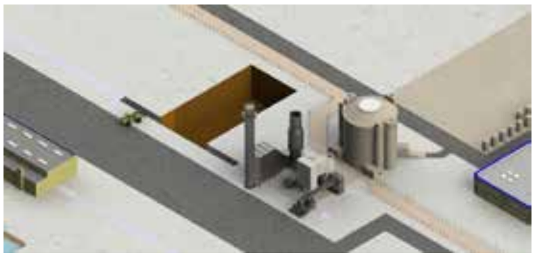

(2) Excavation for the new Mk1 module

(3) Construction of the common tunnel section, for plant utilities

(4) Installation of rails for lift tower

(5) Pour base mat

(6) Install first-level module of Mk1 shield building (SB1)

(7) Install second-level module of Mk1 shield building (SB2)

(8) Install first level of air-duct vault (AD1)

(9) Install second level of air-duct vault (AD2)

(10) Install third level of air-duct vault (AD3)

Fig. 2.8a Storyboard figures for the modular construction process used to assemble a Mk1 PB-FHR unit adjacent to an operating unit.

(11) install Mk1 reactor cavity module (SB4)

(12) Install RV, CTAH and main salt pipes

(13) Install third level module of shield building (SB3)

(14) Back fill below-grade structures to grade

(15) Excavation for next unit may begin

(16) Install main shield building cylinder (SB5)

(17) Install polar crane

(18) Install shield building roof (SB6)

(19) Install DRAC chimneys and ventilation filter and exhaust enclosures (SB7a-g)

(20) Install gas turbine, intake filter housing, generator and main transformer

Fig. 2.8b Storyboard figures for the modular construction process used to assemble a Mk1 PB-FHR unit adjacent to an operating unit.

(21) Install heat recover steam generator and stacks/crane for the next unit is installed and first module for next unit is transferred

(23) Install new protected area fence and remove temporary protected area fence

(22) The lift tower is removed

(24) Unit is assembled and next construction continues

Fig. 2.8c Storyboard figures for the modular construction process used to assemble a Mk1 PB-FHR unit adjacent to an operating unit.

2.4 Mk 1 Steel and Concrete Inputs

The quantities of steel and concrete used to build power plants provide useful data to perform life cycle assessment, as well as input for construction schedule and cost estimates. These quantities were estimated using the SolidWorks model of the plant, to provide a baseline with respect to cost estimation, life-cycle assessment and to determine the size of the lift tower needed to construct a Mk 1 unit. Table 2.1 summarizes the amount of concrete and steel necessary to build a Mk1 unit. Based upon recommendations from Westinghouse, the steel plate used in the structural modules is 1.27 cm thick. The exception is those plates that could experience missile impacts. As a result, the inside of the CTAH vaults and the outside of the above grade surfaces of the shield building use 2.54-cm-thick plates. To estimate the mass of steel in the basemat, the reinforcing steel structure is assumed to use #18 gage rebar. A square lattice has been used that uses a spacing of 0.3 m, with two layers (one at the bottom of the slab, and the other at the top). The air ducts were assumed to use a 2.54-cm-thick cylindrical steel wall. Additionaly, the final steel weight was increased by 10% to account for the weight of tie rods and other fixtures that are used to connect the plates.

The amount of steel used in the reactor building is 28,790 kg/MWe base load, while the quanity of concrete is 240,270 kg/MWe. While the total quantity of steel and concrete needed to build a Mk1 PB-FHR will be larger, it is still interesting that the total is comparable to the 33,000 kg/MWe of steel and 179,500 kg/MWe of concrete that were needed to build 1970's pressurized water reactors (Bryan and Dudley, 1974).

3.0 MAJOR Mk1 REACTOR SYSTEMS

This chapter summarizes the major systems that the Design Integration team considered in developing its shield building and air duct vault designs. A wide variety of systems are required to make the Mk1 PB-FHR, shown in Fig. 3.1, function safely and reliably. At the pre-conceptual level of design, the critical issue for the design of the shield building is to identify major systems that must be located inside the building, to assign space for these systems that is at an appropriate elevation and has appropriate volume to accommodate the equipment. Moreover, the design must consider several additional constraints, including access for equipment installation, inspection and maintenance; ventilation to control transport of hazardous materials; supply for electrical power, cooling, and instrumentation connections; protection from hazards including earthquakes, plane crashes, flooding, and accidental leakage and combustion of natural gas.

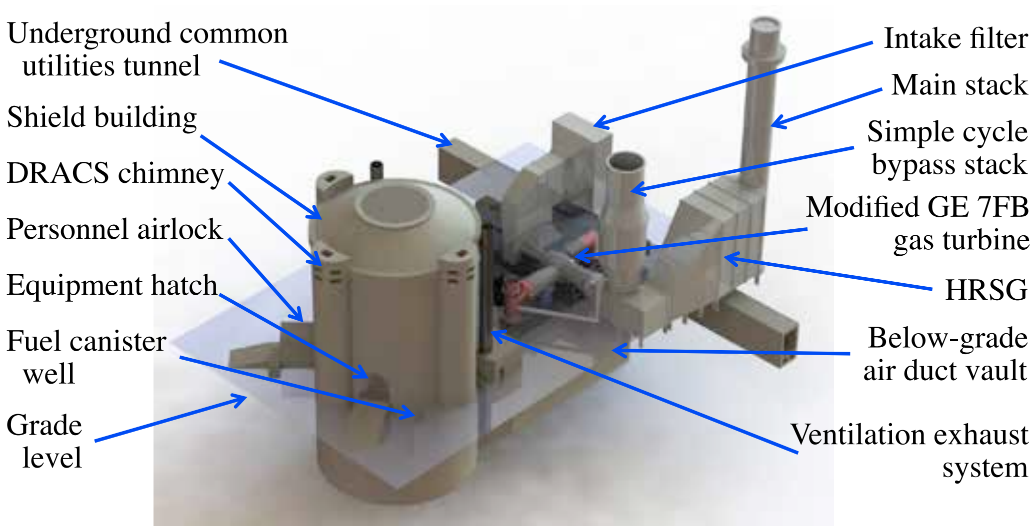

Fig 3.1 Isometric view of the Mk1 shield building and air duct vault structures developed by this design project, and the Mk1 power conversion system.

Since the Mk1 PB-FHR is designed for deployment as a multi-unit plant, some key systems such as the control room and spent fuel storage are shared between units, and therefore are not located inside the reactor shield building. The following subsections describe the major systems that were integrated into the Mk1 shield building and air duct vault designs. Because design information was not available, the Design Integration team developed designs for the Mk1 Polar Crane and for the thermosyphon-cooled heat exchanger (TCHX) of the DRACS system.

3.1 Polar Crane

As with most reactors, the most obvious visual element of the Mk1 reactor building is the high-bay space above the reactor refueling deck. The Mk1 shield building has a polar crane, which provides the ability to lift major equipment components, such as the Mk1 center reflector assembly, up through hatches in the refueling deck floor for removal and replacement. Because the polar crane sweeps the entire area of the high-bay space, chimneys for the DRACS and ducts for the building ventilation system, that extend vertically past the crane elevation, are located on the outside of the shield building.

The polar crane is designed to lift loads, and to lay down tall loads so they can be removed horizontally through the shield building equipment hatch. Replacement of the reactor vessel, if ever required, will occur using an external crane lifting through a hatch in the shield building roof. The cross-beams of the polar crane are separated by 4.5 m so the reactor vessel can be pulled up through the roof hatch in the space between them. The polar crane that was designed for the reactor citadel has been geometrically approximated by a comparison of the two crane beams as a pair of centrally-loaded, simply-supported I-beams to obtain an order of magnitude determination of the required scale for the crane. Each beam of the polar crane was assumed to be able to individually support the maximum expected load to provide an appropriate safety factor. Mass properties that were generated using SolidWorks models of the nuclear heat source were used to calculate the maximum lifting capacity of the polar crane. From these calculations, it has been determined that the polar crane would not be required to lift loads heavier than 100 metric tons (MT). For example, the central and peripheral reflector assemblies, which are constructed of graphite, are calculated to weigh approximately 50 MT.

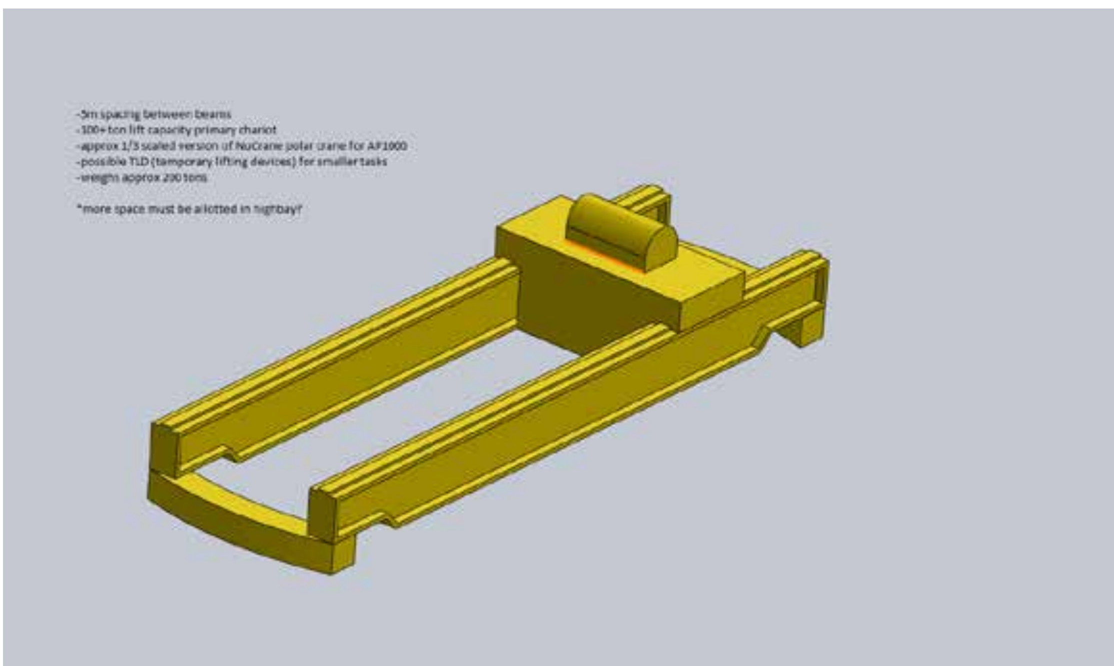

Fig 3.2 100 MT Mk1 polar crane design developed by the Design Integration team.

Using elementary statics theory, the maximum stress in a centrally-loaded, simply-supported I-beam, shown in Fig. 3.3, can be found through the following equation:

$$\sigma_{max} = \frac{Mc}{I} = \frac{Mh}{2I} = \frac{FLh}{4I}$$

where I is the cross-sectional area moment of inertia about the neutral axis, M the loading moment, h the height of beam, F the load, and L the length of crane beams.

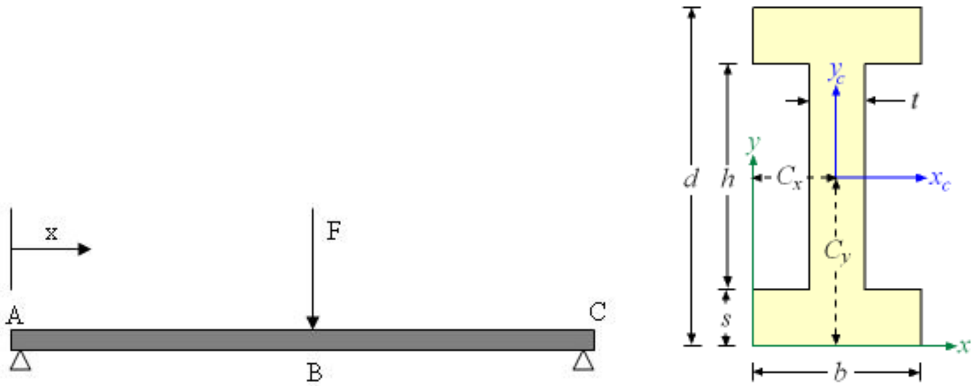

Fig 3.3 Schematic of the beam design for the polar crane (left) and the beam cross section (right).

The diameter of the reactor citadel constrains the length of crane beams L at 22 meters. To obtain the maximum allowable stress σ_{max}, the von Mises yield criterion can be used. Approximating the loading condition at the beam surface as uniaxial stress, the loading criterion $\sigma_{critical}$ reduces to the yield stress σ_{yield}. For a typical structural steel such as ASTM A36 mild steel, $\sigma_{yield} \sim 250$ MPa.

The beam cross-sectional area moment of inertia I is available from the literature, and

$$\sigma_{max} = \sigma_{yield} = \left(\frac{FL}{4}\right)\left(\frac{h}{I}\right)$$

$$\frac{h}{I} = \frac{4\sigma_{yield}}{FL} = 4 \cdot \frac{(250\ \text{MPa})}{(100\ \text{MT})(9.81\ \text{ms}^{-2})(22\ \text{m})} = (46.3\ \text{m}^{-3})$$

The results of the above calculations define a set of constraints or boundary conditions for which the width and height of the polar crane beams was determined. The distance between the beams was set as 5 meters so that the entire reactor vessel can be lifted out between the beams through the hatch on the roof of the reactor citadel using an outside auxiliary gantry crane, if required, although the shield building equipment hatch is also large enough for the vessel to be removed horizontally.

The design of the Mk1 polar crane was scaled from a model designed and manufactured for the AP1000 reactor citadel by NuCrane Manufacturing, LLC. The design of the polar crane also allows for a smaller Temporary Lift Device (TLD) chariot, rated for lower loads for facilitating smaller tasks within the reactor citadel, to be mounted atop the polar crane beams. A similar system employing multiple TLDs has been adopted successfully at EPR Flamanville in France.

3.2 Conical Roof and Upper Shield Building

The design of the conical roof for the Mk1 modules, shown in Fig. 3.4, has been inspired from advice from Westinghouse, which uses a similar design for the roof of the AP1000 shield building, to provide greater strength compared to the flat cylindrical roof in the Mk1 previous design (Fig. 2.2). The roof fits inside the stiffening ring at the top of the shield building cylindrical wall, and implements a 30-degree angle for higher structural integrity compared to the previous design.

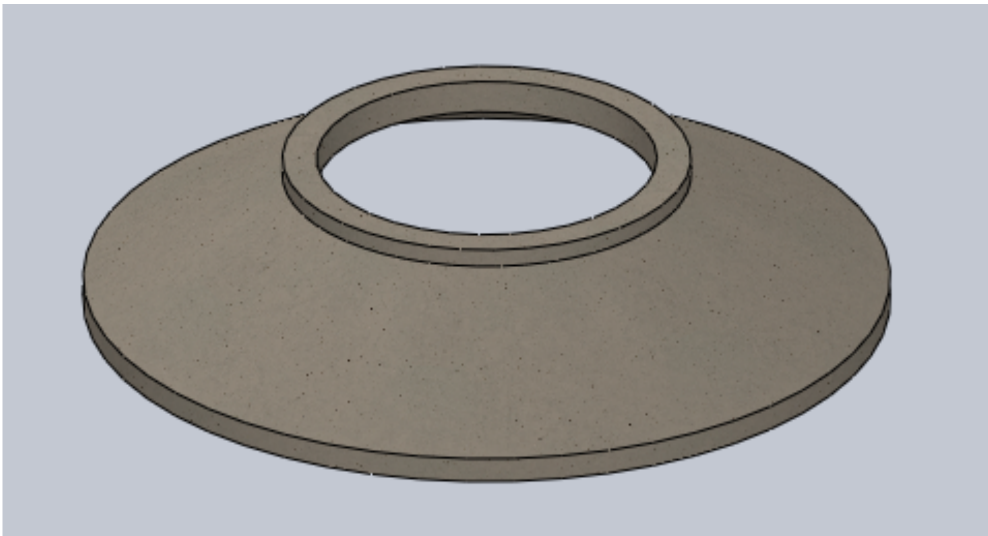

Fig 3.4 Mk1 conical shield building roof.

The conical roof design is a multifunctional feature that enables the above-grade structures of the shield building, shown in Fig. 3.5, to function effectively for all weather environments (rain, snow, and environmental considerations such as natural debris collecting on a flat surface). All of these natural causes could lead to increased stress and constriction of the DRACS and ventilation systems. Additional considerations include the possible impact of commercial aircraft, where using a design scaled from the AP1000 provides the initial basis to achieve similar performance.

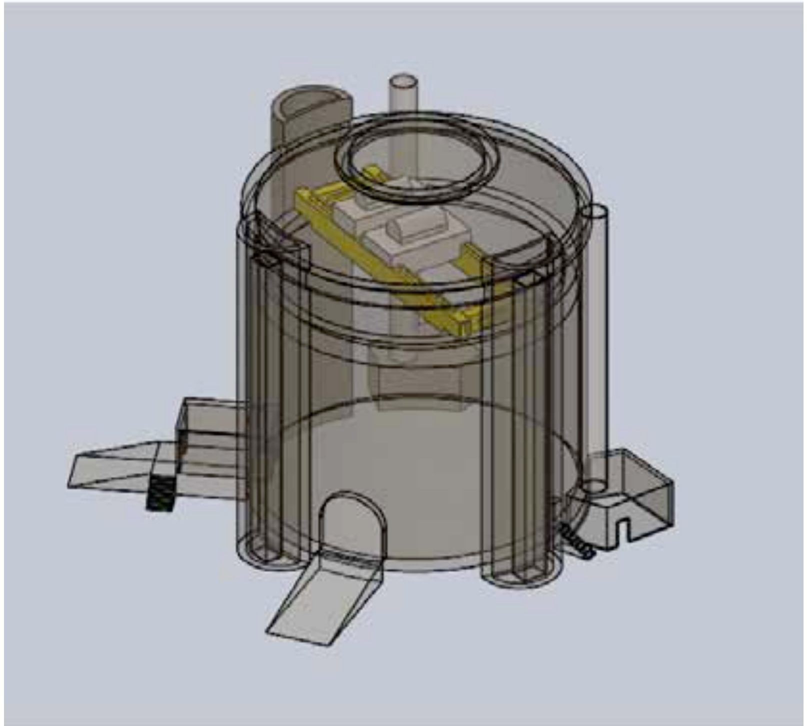

Fig 3.5 Mk1 above-grade shield building.

3.3 Ventilation System

The Mk1 design has a low-leakage containment, with a filtered confinement system around the containment to provide an additional barrier to radionuclide release and to protect personnel from exposure to hazardous chemicals (particularly beryllium from the salt coolant) and radionuclides. The Mk1 ventilation system is configured to progressively transfer air from cleaner areas to potentially more contaminated areas.

The Mk1 air handling equipment is located in grade-level structures next to the shield building. External air is filtered and introduced through diffusers into the top of the shield building high-bay space, where it then flows through vents in the refueling deck downward to areas with higher potential levels of contamination. Exhaust air from these potentially more contaminated volumes is collected, and flows up through a duct on the outside of the shield building to an exhaust system on the top of the shield building where the air is monitored for contamination, filtered, and exhausted to a discharge stack. A similar, separate system provides ventilation for the air duct vault.

3.4 Reactor Cavity, Thermal Shield, Cover Gas and Containment Systems

The Mk1 PB-FHR uses a low-leakage, low-pressure containment. Because the PB-FHR coolant has very low vapor pressure and low chemical reactivity, the only mechanism to increase pressure in the containment is heating of the cover gas. To minimize the pressure increase from cover gas heating, the larger volume of the cover gas handling system is included inside the primary containment boundary.

The Mk1 design uses a refractory cavity liner system (Andreades et al., 2014), where ceramic insulation blocks in the reactor cavity minimize the free volume between the reactor vessel and the cavity liner plate, so that the drop in the salt level in the reactor vessel is minimized if the vessel leaks or ruptures.

This project did not perform any detailed design of the thermal shield or cover gas handing system, but it did assure that the shield building design provides appropriate space for these systems.

3.5 DRACS

The Mk1 design uses three modular DRACS units for emergency decay heat removal, when the normal shutdown cooling system is not functional. The DRACS are passive and function by natural circulation. Each module consists of a DRACS heat exchanger (DHX) located inside the reactor vessel, a DRACS salt loop, a thermosyphon-cooled heat exchanger (TCHX) outside the reactor containment, which transfers heat from the DRACS salt loop to evaporate water, a water thermosyphon, an air cooled condenser, a natural draft chimney to provide air flow to the condenser, and a water storage tank.

The DHX, the DRACS loop, the TCHX and their salt fill tank, shown in Fig. 3-6, are designed to be a single module that can be factory fabricated, and installed and replaced through a hatch in the refueling deck (Andreades et al., 2014). The DRACS water pools are designed to have a sufficient reserve volume of water to accommodate early boil-off immediately after reactor shutdown when decay heat levels are high, and to provide gravity driven flow to the TCHXs.

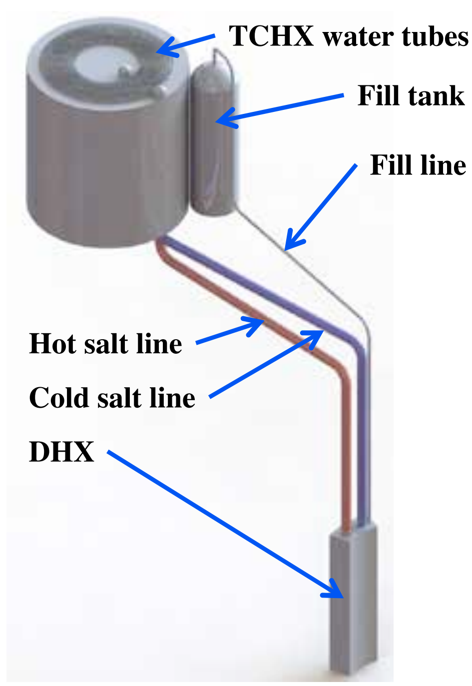

Fig 3.6 Isometric view of the DHX and TCHX for the Mk1 PB-FHR.

3.5.1 DHX

The DHX transfers heat from the primary loop to the DRACS loop. It is a counter-flow, single pass, twisted tube heat exchanger with a 0.56-m-diameter, 2.5-m-high shell, and tubes arranged in a triangular pattern with a 1.25 pitch-to-diameter ratio. The DHX uses 984 tubes, and each of them is 0.0127 m in diameter.

3.5.2 TCHX

The TCHX transfers heat from the DRACS salt loop to a water themosyphon loop. Heat transfer between the DRACS salt and water is mainly by thermal radiation. The schematic for heat transfer from salt to water is shown in Fig. 3.6.

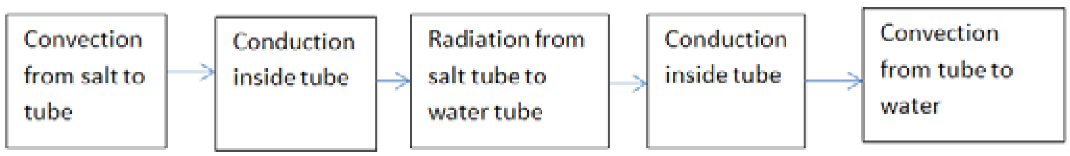

Fig 3.6 Schematic of heat transfer in the TCHX.

One important task of our team was to design the TCHX, for which no preliminary design existed, based on required thermal load (2.36 MWt for each DRACS), fluid properties and space constraints. Details of the calculations leading to a final TCHX design are provided in Appendix A.

The final design uses 9 salt tube bundles stacked vertically, arranged in a helical, conical shape, and vertical thermosyphon water tubes. A hot salt inlet manifold with a head tank distributes salt from the outer radius of the TCHX, the salt flows inwards and downwards in the salt tube bundles, and it is collected in a cold salt manifold pipe before returning to the DHX through the DRACS loop.

Figure 3.7 shows the top view of one bundle of the TCHX and Fig. 3.8 shows an isometric view of all 9 bundles of the TCHX.

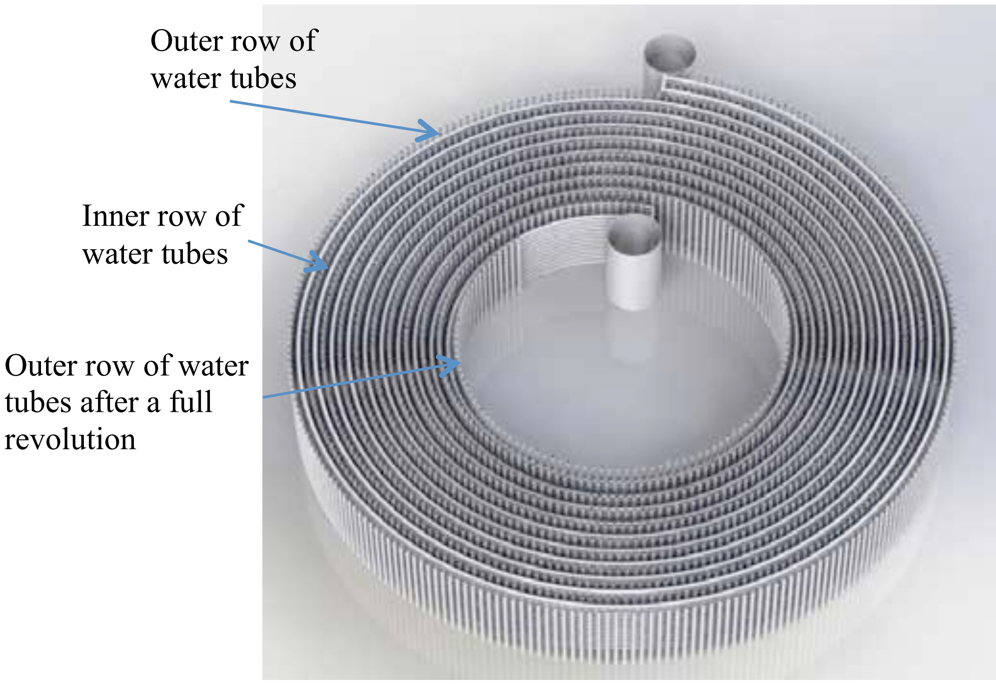

Fig 3.7 Top view of a single bundle in the TCHX developed by the Design Integration team.

Fig 3.8 Isometric view of the TCHX salt and water tubes.

In the SolidWorks model of the TCHX, the distance from the center of the heat exchanger to the edge of the hot manifold pipe is 1.104 m. Therefore, the radius of the TCHX shell is chosen to be 1.11 m. Because of space constraints, the height of the TCHX is designed to be 2.6 m.

Future modifications are expected to develop a complex manifold system to supply and collect water to/from the thermosyphon water tubes, so that they can be activated in banks. For now, the tubes are simply shown protruding from the top and bottom of the TCHX shell.

3.6 Fuel Handling

The Mk1 reactor has a fuel handling system located in a shielded cell adjacent to the reactor cavity. Figure 3.9 shows the space in the Mk1 shield building that was dedicated to the fuel handling function, along with a transfer air lock that allows fuel canisters to be introduced or removed from the cell, to a canister transporter vehicle that drives above the airlock.

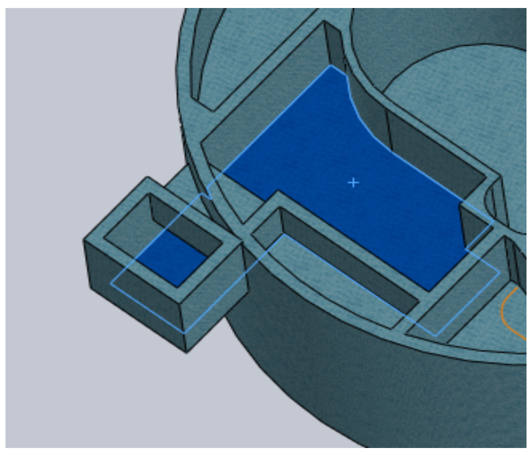

Fig 3.9 Mk1 fuel handling area and canister transfer airlock.

3.7 Service Cooling Water and Sumps

The Mk1 reactor cavity liner uses water cooling (Andreades et al., 2014). Air handling and other equipment inside the shield building is also water-cooled. The service water system provides this cooling, and rejects heat through service water heat exchangers to cooling tower water supplied from the common services tunnel. The service water cooling system has three independent 50% capacity trains of heat exchangers and pumps to provide cooling water.

Under accident conditions, the service water system is configured to provide cavity cooling by boiling of water, and it has water storage tanks, with a tank-in-tank design to facilitate detection and containment of leaks of sufficient capacity and elevation to provide extended cooling capacity to the cavity liner cooling system by boiling of water.

The use of water inside the shield building creates the potential for leaks. The air duct vault and shield building both have sump systems to collect leaked water from areas where water-cooled equipment and water piping are located. This includes water released into the drain chases around the cavity liner cooling tubes. Under beyond design basis accident conditions, flooding of these sumps can fill the cavity-liner drain chases with water, and thus provide a heat removal path from the reactor cavity if all other paths have been disabled.

3.8 Electrical Power and Instrumentation

The Mk1 shield building houses equipment with numerous electrical and instrumentation requirements, including various pump and blower motors, as well as cavity and salt pipe heating systems. It will also include sampling and monitoring systems for components within the reactor and coolant circulation loop such as temperature, pressure, leakage rate, and radiation.

3.9 CTAH and Air Duct Vault

The Mk1 design places the CTAHs and their air ducts in a below-grade vault. Because the possibility exists that fuel gas could leak into the ducts or these vaults and ignite, the vaults for the high pressure and low pressure ducts are separated, have grade-level blow-out panels to control over-pressure, and have hardened walls between the CTAHs and the reactor building to protect equipment in the reactor building.

This section describes the structural modules that are used to build the Mk 1 air duct vault. The design of the structural modules plate thicknesses and geometry are based upon advice provided by Westinghouse. In order to protect the equipment and the structural integrity within the reactor building in preparation for the probability of a natural gas over-pressure or explosion, the air duct vault was designed to use reinforced walls between the CTAH enclosures and the main-salt equipment inside the shield building, so that over-pressure or damage in the air duct vault or CTAH enclosures will not affect safety-related equipment inside the shield bulding. To this effect, we added thicker outer steel plate and concrete between the CTAH and the main-salt system. Because the CTAHs are heated by flibe, they provide a potential source of beryllium contamination. The ventilation system in the air duct vault is configured to progressively transfer air from the area with lowest level of beryllium contamination to more contaminated area, with the flow finally entering into the CTAH enclosures and then being removed through the air duct vault exhaust fan and filter system.

The air duct 1 (AD1) module is installed with the air ducts already located within the module, as seen in Fig. 3.10. It will also have space allocated for auxiliary equipment, which will include an air monitoring system since this is where the air will leave the complete air duct system, leading to the exhaust fan and filter system located at ground level adjacent to the shield building. There is additional space for other components, such as sump system, that the Design Integration team has not designed or located in the timeframe of this project. The AD1 module creates the ground floor of the air duct vault, which sits on the base mat. The module also contains a stairwell, sized to match typical stairwells in reactors such as the Advanced Boiling Water Reactor, which allows access from the two upper air duct vault modules to allow for typical maintenance and system management of the auxiliary equipment housed there. The center panel on the top face of this module is designed as an equipment hatch that also acts as a blow-out panel to relieve pressure if a natural gas leak and explosion were to occur inside the vault or the air duct.

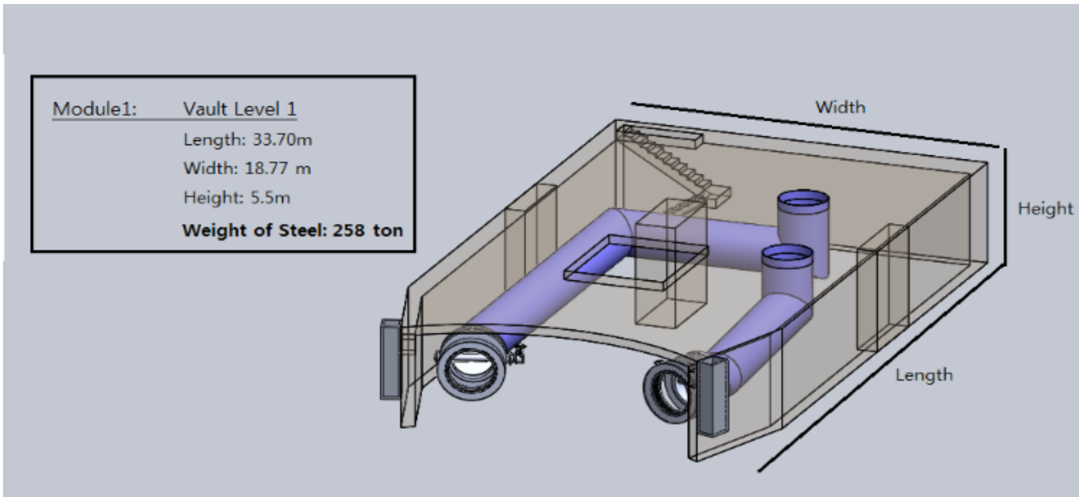

Fig 3.10 AD1 module with pre-installed air ducts.

Figure 3.11 shows the AD2 module. This module will have significantly more space than AD1 and AD3 for auxiliary components and equipment. Space is primarily allotted to the systems required to maintain positive air pressure in the entire air duct vault system. The air flow system to keep the 3rd level at the lowest pressure with the 2nd and 1st at increasing pressures would be immense. In comparison, the air handling system that is currently in use at the General Electric Vallecitos hot cell facility is approximately the same size volumetrically and could be considered to maintain the air flow requirements of the air duct vault. A backup diesel generator or engine could also be housed to provide backup power to the critical systems in an emergency situation. This module also has an equipment hatch that is aligned with the AD1 and AD3 equipment hatches to provide an accesses point to all levels within the air duct vault for construction and repair purposes.

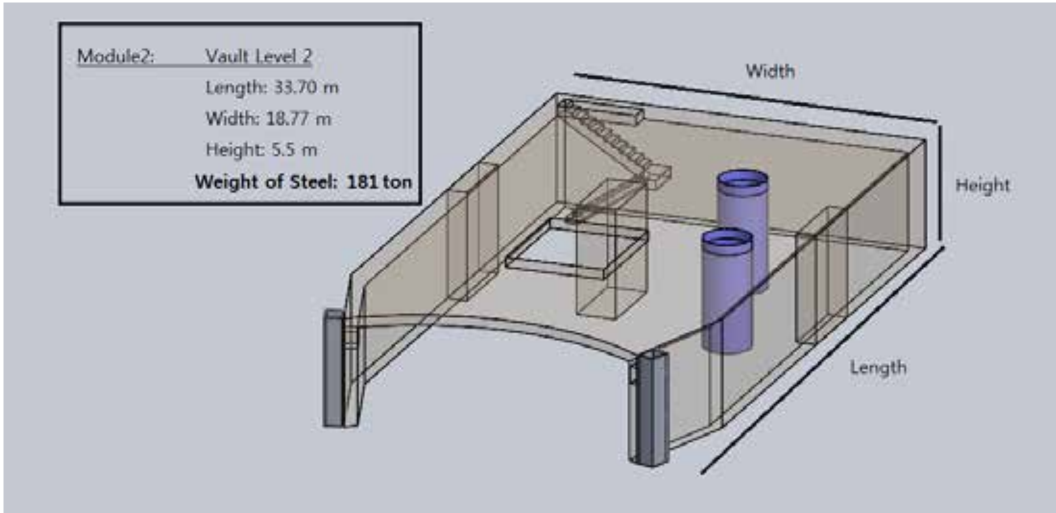

Fig 3.11 AD2 module.

The AD3, shown in Fig. 3.12, is the last of the air duct vault modules to be installed. It has been designed for the location of the turbine, and the structure that runs perpendicular to the longest side is the turbine pedestal. In the back left corner, there is a separate personnel hatch that allows access of the air duct vault from the top of the air duct system without having to use the common services tunnel. Installment of this unit will include the turbine pedestal, the hot and cold legs of tubing air ventilation system that transfers the air coming from the first AD module and connects it to the penthouse. Additionally, the AD3 module allows access from the common services tunnel to the air duct vault system and will also be used to transport equipment in the installation of final components and to allow for the pertinent maintenance required for a natural gas facility with constraints on the access allowed to the shield building.

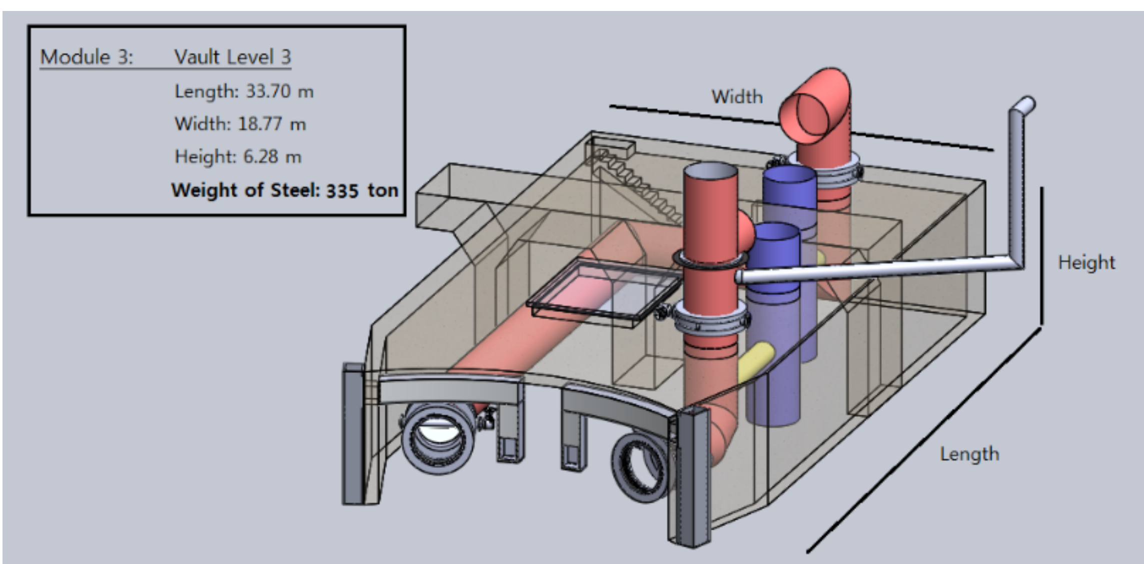

Fig 3.12 AD3 module.

Figure 3.13 shows a plan view of the combined air duct vault, shield building, and common underground tunnel modules at the AD3 level.

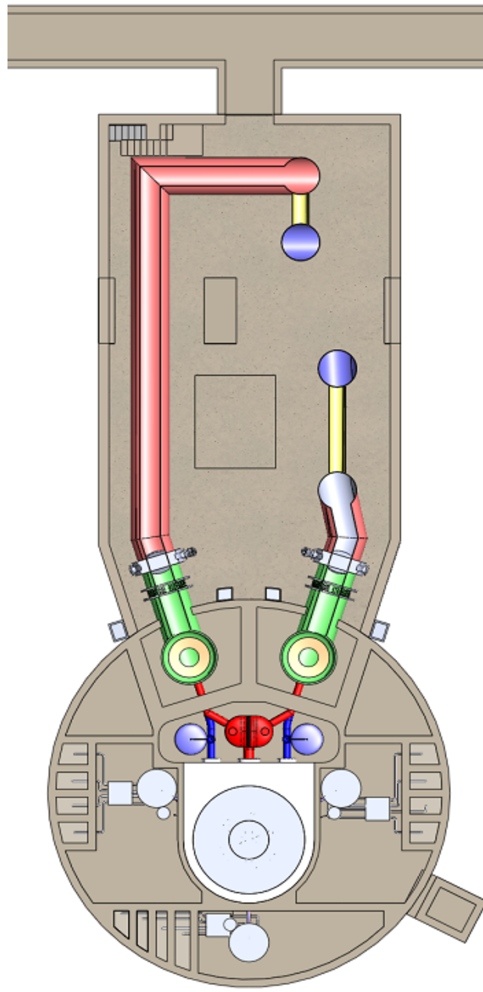

Fig 3.13 Top cross-sectional view of Mk1 showing the shield building and air duct vault.

The protected area of the Mk1 reactors is separated from the power conversion equipment and the remainder of the owner controlled area by a double fence, which enables detection of unauthorized access into the protected area by using sensors to detect intruders crossing between the fences. Figure 3.14 shows the configuration of the fences adjacent to the shield building of a Mk1 unit. Below grade, there are no portals or access paths between the shield building and the air duct vaults, which prevents unauthorized access.

Fig 3.14 Top cross-sectional view of Mk1 showing the shield building and air duct vault.

3.11 Other Systems

The systems that should also be considered are fire protection, space for heavy load handling equipment and tools other than polar crane, coolant-draining system. Other mechanical handling systems should also be considered such as different types of hoists.

4.0 SUMMARY

This design project, to develop the reactor building for the Mk1 PB-FHR, required extensive coordination with subject matter experts on various aspects of the Mk1 design, and multiple iterations to develop an integrated design that can be constructed using SC structural modules and modular construction methods like the AP1000. The resulting design uses quantities of steel and concrete, per megawatt of base load capacity, that are similar to the quantities needed to build large, advanced LWRs. This suggests that the Mk1 PB-FHR may have attractive economics.

5.0 REFERENCES

D. Ambrose, 2014, "3.4.2 Vapour pressure of water at temperature between 0 and 360^{o}C," NPL National Physical Laboratory, http://www.kayelaby.npl.co.uk/chemistry/3_4/3_4_2.html (3-21-2014)

C. Andreades, et al., 2014, "Technical Description of the 'Mark 1' Pebble-Bed Fluoride-Salt-Cooled High-Temperature Reactor (PB-FHR) Power Plant," Department of Nuclear Engineering, U.C. Berkeley, Report UCBTH-14-002, 2014.

R.H. Bryan and I.T. Dudley, 1974, "Estimated Quantities of Materials Contained in a 1000-MW(e) PWR Power Plant," Oak Ridge National Laboratory, ORNL-TM-4515.

J. Buongiorno, 2010, "Notes on two phase flow, boiling heat transfer, and boiling crises in PWRs and BWRs." MIT Department of Nuclear Science and Engineering, Fall 2010.

A. Chaudhuri, R. Kuo, J.H. Lee, and A. Lubbers, 2014, "NE-170 Radiation protection and shielding in the Mk1 PB-FHR reactor," Department of Nuclear Engineering, U.C. Berkeley, Report UCBTH-14-006.

F.P. Incropera, David P. Dewitt, 2012, *Fundamentals of Heat and Mass Transfer*, seventh edition, Jefferson City: John Wiley & Sons. (pp. 519-530, 824, 866-885)

P.F. Peterson, 2010, "Appendix C: Property Values" in *Thermal Aspect of Nuclear Reactors* by Per F. Peterson. Course Notes for NE260-Fall, 2010. (pp. 275-291)

P.F. Peterson, "Convective Boiling" in *Thermal Aspect of Nuclear Reactors* by Per F. Peterson. Course Notes for NE260-Fall, 2010. (Chapter 13, pp. 207-233)

APPENDIX A – TCHX SIZING

This appendix provides details of the sizing method for the thermosyphon cooled heat exchanger (TCHX), following the heat transfer mechanisms listed in Fig. 3.6.

As a first approximation, it is assumed that the heat fluxes on both salt and water sides are uniform but not necessarily the same. As a result, the Nusselt number (Nu) is 4.36 for convection heat transfer on the salt side (fully developed laminar flow). The equation that relates thermal conductivity of the fluid (k) and convection heat transfer coefficient (h) inside the tubes is

$$Nu = \frac{hD_i}{k} = 4.36 \tag{1}$$

where D_i is the inner diameter of the tube. For the salt flow to be in the laminar regime, the Reynolds number (Re) must be 2300 or less (Incropera & Dewitt, 2012). The Reynolds number is given as:

$$Re = \frac{D_i}{\mu_s} * v_s \rho_s = \frac{D_i}{\mu_s} * \frac{m_s 4}{D_i^2 \pi n_s} \leq 2300 \tag{2}$$

where v_s is the salt velocity and n_s is the number of salt tubes. Solving for n_s, a minimum of 63 salt tubes is needed for the salt flow to be in the laminar regime. The maximum hydrodynamic entry length for laminar flow is expressed as (Incropera & Dewitt, 2012):

$$x_{fd,d} = 0.05 Re * D_i = 0.05 \frac{D_i}{\mu_s} * \frac{m_s 4}{D_i^2 \pi n_s} D_i = 0.2 \frac{m_s}{\pi n_s \mu_s} \tag{3}$$

Convection from salt to tube

The equation for convection heat transfer is:

$$q = A_{s,i} h_s \left(T_{s,m} - T_{s,i}\right) = \pi D_i n_s L_s \frac{4.36 * k_s}{D_i} \left(T_{s,m}(x) - T_{s,i}(x)\right) = 4.36 \pi n_s L_s k_s \left(T_{s,m}(x) - T_{s,i}(x)\right) \tag{4}$$

where $A_{s,i}$ is the inner surface of the salt tubes, h_s is the convection heat transfer coefficient, L_s is the total length of salt tubes, $T_{s,m}(x)$ is the bulk salt temperature as a function of linear coordinates along the tube, and $T_{s,i}(x)$ is the temperature of the inner surface of the tube as a function of linear coordinates along the tube. Equation (5) gives $T_{s,m}$ as a function of inlet salt temperature $T_{s,in}$ and x (Incropera & Dewitt, 2012):

$$T_{s,m}(x) = T_{s,in} - \frac{q \pi D_i}{A_{s,i} m_s C_p} x = T_{s,in} - \frac{q}{L_s m_s C_p} x \tag{5}$$

where x is the linear coordinate along the salt tube. Because $T_{s,m}$ is changing along the tube, the temperature of the inner surface of the tube, $T_{s,i}$, is also changing to yield a uniform heat flux ($T_{s,m} - T_{s,i}$ is uniform).

Conduction inside salt tube

The equation for conduction is (Incropera & Dewitt, 2012):

$$q = 2\pi n_s L_s k_{s,pipe} \frac{T_{s,i}(x) - T_{s,o}(x)}{ln(D_o/D_i)} \tag{6}$$

In equation (6), $T_{s,o}$ is the temperature at the outer surface of the salt tube. Since $T_{s,i}$ is changing along the salt tube, $T_{s,o}$ is also changing to yield a uniform heat flux ($T_{s,i} - T_{s,o}$ is uniform).

Radiation from salt tube to water tube

The equation for heat transfer by radiation is (Incropera & Dewitt, 2012):

$$q = \frac{\sigma({T_{s,o}}^4 - {T_{w,o}}^4)}{\frac{1-\epsilon_S}{\epsilon_S A_{s,o}} + \frac{1}{A_{s,o}F} + \frac{1-\epsilon_W}{\epsilon_W A_{w,o}}} \tag{7}$$

In equation (7), $T_{s,o}$ is approximated as the average temperature of the outer surface of the salt tube, $T_{w,o}$ is the temperature of the outer surface of the water tube, F is the view factor from salt tubes to water tubes, and $A_{s,o}$ and $A_{w,o}$ are the outer surface areas of the salt tubes and water tubes, respectively. In equation (7), $A_{s,o}$ and $A_{w,o}$ can be calculated as:

$$A_{s,o} = \pi D_o n_s L_s \tag{8}$$

$$A_{w,o} = \pi D_o L_{TCHX} n_w \tag{9}$$

In equation (9), n_w is the total number of water tubes. In equation (7), it is assumed that the tubes are opaque, diffuse and grey surfaces. With this assumption, the absorptivity and emissivity of the water tubes are equal, and assuming that the water tubes are painted black, their emissivity and absorptivity can be as high as 0.95 (Incropera & Dewitt, 2012).

Assuming the configuration of the salt tubes and water tubes can be considered similar to the case where radiation originates from an infinite plane (salt tubes) and is incident to a row of cylinders (water tubes), the equation for the view factor (F) is (Incropera & Dewitt, 2012):

$$F = 1 - \left[1 - \left(\frac{D_o}{s}\right)^2\right]^{0.5} + \left(\frac{D_o}{s}\right) tan^{-1}\left(\left(\frac{s^2 - {D_o}^2}{{D_o}^2}\right)^{0.5}\right) \tag{10}$$

where s is the distance between the center of a cylinder and the center of the next cylinder (center-to-center distance between water tubes in this case).

Conduction inside water tube

The equation for conduction is

$$q = 2\pi n_w L_{TCHX} k_{w,pipe} \frac{T_{w,o} - T_{w,i}}{ln(D_o/D_i)} \tag{11}$$

In equation (11), $T_{w,i}$ is the temperature at the inner surface of the water tube.

Convection from tube to water

The equation for convection heat transfer is:

$$q = A_{w,i} h_w \left(T_{w,i} - T_w\right) = \pi D_i L_{TCHX} n_w h_w \left(T_{w,i} - T_w\right) \tag{12}$$

In equation (12), h_w is either the 1-phase or 2-phase convection heat transfer coefficient. The phase of water inside each vertical tube is determined by enthalpy, a function of height, given as (Buongiorno, 2010):

$$h(z) = h_{in} + \frac{q}{m_w L_{TCHX}} * z \tag{13}$$

where h_{in} is water enthalpy at the inlet of the tubes and z is the vertical coordinate along the tube. If the water is in the 2-phase regime, then h_w is calculated as (Peterson, 2010):

$$h_w = h_c + h_{NB} \tag{14}$$

where h_c is the convection heat transfer coefficient and h_{NB} is the contribution from nucleate boiling.

$$h_c = 0.023 \left(\frac{G(1-\chi)D_i}{\mu_f}\right)^{0.8} (Pr_f)^{0.4} \frac{k_f}{D_i} F_h \tag{15}$$

$$h_{NB} = S(0.00122) \left(\frac{k_f{}^{0.79} C_{p,f}{}^{0.45} \rho_f{}^{0.49}}{\sigma_w{}^{0.5} \mu_f{}^{0.29} h_{fg}{}^{0.24} \rho_g{}^{0.24}}\right) (T_{w,i} - T_{sat})^{0.24} (p_{w,i} - p_{sat})^{0.75} \tag{16}$$

$$F_h = 1 \quad for \ \frac{1}{X_{tt}} < 0.1 \tag{17}$$

$$F_h = 2.35 \left(0.213 + \frac{1}{X_{tt}}\right)^{0.736} \quad for \ \frac{1}{X_{tt}} > 0.1 \tag{18}$$

$$\frac{1}{X_{tt}} = \left(\frac{\chi}{1-\chi}\right)^{0.9} \left(\frac{\rho_f}{\rho_g}\right)^{0.5} \left(\frac{\mu_g}{\mu_f}\right)^{0.1} \tag{19}$$

$$S = \frac{1}{1+2.53*10^{-6}(Re_{2\Phi})^{1.17}} \tag{20}$$

$$Re_{2\Phi} = F_h{}^{1.25} G(1-\chi) \frac{D_i}{\mu_f} \tag{21}$$

$$G = \frac{m_w}{\pi \frac{D_i{}^2}{4} n_w} \tag{22}$$

χ is the flow quality, which is determined by:

$$h = (1-\chi)h_f + \chi h_g \tag{23}$$

where h is calculated from equation (13). In equation (16), $p_{w,i}$ is the water vapor pressure determined at $T_{w,i}$. One correlation for $p_{w,i}$ is (Ambrose, 2014):

$$p_{w,i} = p_c * \exp(a_1\tau + a_2\tau^{1.5} + a_3\tau^3 + a_4\tau^{3.5} + a_5\tau^4 + a_6\tau^{7.5}) * \frac{T_c}{T_{w,i}} \tag{24}$$

$$\tau = 1 - \frac{T_{w,i}}{T_c}$$

where a_1= -7.85951783, a_2= 1.84408259, a_3= -11.7899497, a_4= 22.6807411; a_5= -15.9618719, a_6= 1.80122501, T_c= 647.096 K, and p_c= 22064000 Pa.

Configuration

The salt tubes are arranged in a helical, conical shape. The equations that describe this shape are:

$$x_1(t) = a_1 * t * \cos(w * t) \tag{25}$$

$$y_1(t) = a_1 * t * \sin(w * t)$$

$$z_1(t) = t$$

where t ranges from z_0 to $2.5/n+z_0-H$ with n being the number of bundles stacked vertically and H the height of one bundle. With the given range of t, each tube can fit into one bundle with a height of $2.5/n$ [m]. The radius of the coil reaches its maximum value (R) when t is equal to $2.5/n+z_0-H$. $cos(w*t)$ is equal to 1 at that t, therefore a_1 is given by:

$$a_1 = \frac{R}{\frac{2.5}{n}+z_0-H} \tag{26}$$

We call "gap" the radial distance between each loop of the coil:

$$gap = x_1\left(\frac{2.5}{n} + z_0 - H\right) - x_1\left(\frac{2.5}{n} + z_0 - H - \frac{2\pi}{w}\right) \tag{27}$$

Δt needed to make one full rotation along the coil is:

$$\Delta t = \frac{gap}{a_1} \tag{28}$$

From equation (28), w is given by:

$$w = \frac{2\pi}{\Delta t} \tag{29}$$

The linear position along the coil is given by:

$$S(t) = \frac{t}{2}\sqrt{1 + {a_1}^2(1 + (w*t)^2)} + \frac{1+{a_1}^2}{2*a_1*w} sinh^{-1}\left(\frac{a_1*w*t}{\sqrt{1+{a_1}^2}}\right) \tag{30}$$

$S(2.5/n+z_0-H)-S(z_0)$ should be equal to the salt tube length L_s. With this, z_0 will be determined and the inner radius of the bundle is a_1*z_0.

The water tubes are arranged between the salt tubes. Viewed from the top, they follow a spiral of equation:

$$r(\theta) = a_2 + b_2 * \theta \tag{31}$$

where a_2 is the starting radius and b_2 is the spatial frequency. If the water tubes spiral starts at $r(\theta = 0) = a_1 * z_0 - gap/2$ and for each full revolution, the radius of the spiral increases by gap (i.e. $r(2\pi + \theta) - r(\theta) = gap$), then a_2 and b_2 are given by:

$$a_2 = a_1 * z_0 - gap/2 \tag{32}$$

$$b_2 = \frac{gap}{2\pi}$$

If the maximum radius of the spiral is R, then

$$\theta \in \left[0, \frac{R - a_2}{b_2}\right]$$

The total length of the water tubes spiral is then given by:

$$L = \int_0^{\frac{R-a_2}{b_2}} \sqrt{r^2 + \left(\frac{dr}{d\theta}\right)^2} d\theta \tag{33}$$

The number of water tubes that fit in the spiral is L/s, where s is the center-to-center distance between each water tube.

Calculation

The TCHX has n tube bundles stacked vertically. Each bundle has n_s/n salt tubes and transfers a power of q/n to water pipes with a length of L_{TCHX}/n. The approach for size calculation is:

1. Guess n_s, L_s, n_w, ε_w, s, and n
2. Combine equations (1-12) into one equation to determine h_w
3. Solve for h_w and compare with value from equation (14)
4. If h_w does not match value from equation (14), then return to step 1

Results

Assuming that the temperature of the salt tubes outer surface is averaged along the tubes and the tubes are opaque, diffuse and grey surfaces, a Matlab code was used to calculate the parameters required for the heat exchanger. Iteration was performed as follows to get to the final results:

1. Guess s such that the view factor between salt tubes and water tubes, calculated using equation (10), is approximately the same as a preliminary estimated value of 0.7
2. Guess initial n_s, then calculate L_s using equation (8) and assuming that the total area of salt tubes needed is 203 m^2 [1]
3. Guess ε_w, n_w and n, then calculate for h_w with equations (1-12)
4. Keep s, n_s, area of salt tubes, n_w, and ε_w the same while changing n; results in equations (1-14) do not change when n changes
5. Keep n, area of salt tubes, n_w, ε_w and s the same while changing only n_s; results in equations (1-14) do not change when the salt tubes area is kept constant
6. Keep other parameters constant while changing the area of salt tubes and n_w in each bundle until equation (7) has a real solution when solving for $T_{w,o}$
7. To make h_w more closely match the value from equation (14), change the length of salt tubes in each bundle (this also changes the area of salt tubes)
8. Finally, change s and solve for h_w using equations (1-14); if the result is imaginary, guess different s such that $F*A_{s,o}$ remains approximately constant, and return to step 1.

Table A-1 lists important result parameters for the TCHX.

Table A-1. Parameters for the TCHX.

Parameter	Symbol	Value	Unit
Number of salt tubes	n_s	234	
Number of water tubes	n_w	1990	
Individual salt tube length	L_s	24	m
Water tubes emissivity	ε_w	0.95	
Distance between centers of water tubes	s	0.0254	m
View factor	F	0.6576	
Number of bundles stacked vertically	n	9	
Hydrodynamic entry length	$x_{fd,d}$	0.34	m
Total outer area of salt tubes	$A_{s,o}$	224.11	m^2

Figure 3.7 shows a plot of h_w calculated from equations (1-12) and equation (14).

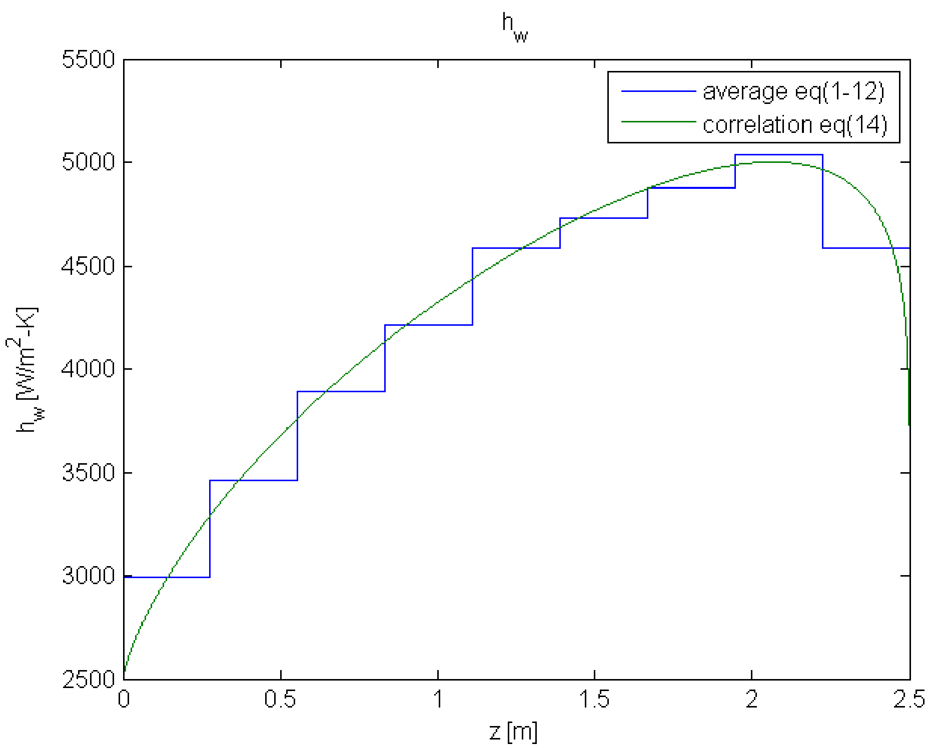

Fig A-1 Heat transfer coefficient from water tubes to water, from equations (1-12) and equation (14).

A Matlab code was used to simulate the shape of one salt tube and determine whether 1990 water tubes can fit with an average salt tube length of 24 m. The results from the simulations are provided in Table A-2.

Table A-2. Parameters for heat exchanger configuration.

Parameter	Symbol	Value	Unit
Outer coil radius	R	0.89	m
Radial distance between consecutive coils	gap	0.1016	m
Height of stack of salt tubes	H	0.2383	m
Inner coil radius		0.1276	m
Number of water tubes that can fit		2035	